

Sn foil as cathode for a reversible 2.8 V Sn-Li battery

*Kaiming Xue, Yu Zhao, Pui-Kit Lee, Denis Y. W. Yu**

School of Energy and Environment, City University of Hong Kong, 83 Tat Chee Ave,
Kowloon, Hong Kong

E-mail: denisyu@cityu.edu.hk

Experimental

Cell configuration and assembly

The preparation process of the anion exchange membrane was adopted from our previous work¹ with slight modification. Specifically, a 45 wt% solution of poly(ionic liquid) (PIL) with poly(diallyldimethylammonium bis(trifluoromethanesulfonyl)imide) (PDADMATFSI) in N-methyl-2-pyrrolidone (NMP) solvent was coated on commercial PP membrane (Celgard 2400) via a doctor blade with a 50 μm gap. The NMP solvent was then removed from the coated separator (PIL/PP) by drying on a hotplate at 65 °C.

Rectangular Sn foil with the size of 2 cm \times 2.5 cm and a thickness of 60 μm was used as the cathode, which was coupled with Li metal anode and assembled into a Al-laminated pouch cell with the PIL/PP separator sandwiched between two pieces of glass fiber sheets (Advantec #GD-120, thickness 0.51 mm) in an Ar-filled glovebox (contents of H₂O and O₂ smaller than 0.1 ppm). The function of two glass fiber sheets was to hold larger amount of electrolyte solution in the cell. Two Ni tabs were used to connect the cathode Sn foil and anode Li foil to the outside testing equipment. 2 ml of 3 M LiTFSI (lithium bis(trifluoromethanesulfonyl)imide) in mixed solvent composed of 1,2-dimethoxyethane (DME) and propylene carbonate (PC) was used as the electrolyte

solution. The volume ratio of DME and PC in the mixed solvent was 50% to 50%. 1 ml electrolyte was used as the catholyte and the other 1 ml electrolyte was utilized as the anolyte.

For comparison, Cu-Li and Ni-Li batteries were also assembled with Cu foil and Ni foil with the same size as the Sn foil. All other parameters such as separator, anode, electrolyte, etc. of the Cu-Li and Ni-Li batteries were the same as those used in the Sn-Li battery.

Electrochemical and materials characterizations

In order to investigate the redox reactions in the Sn-Li battery, the battery was charged under a current density of 1 mA cm^{-2} (5 mA) to the areal capacity limitation of 4 mAh cm^{-2} (20 mAh) and then discharged to 1.5 V. The crystal structure of Sn cathode foils at different states were examined with X-ray Diffraction (XRD) (PANalytical X'Pert3 X-ray Diffractometer, Cu K_{α} , $\lambda = 1.5418 \text{ \AA}$). The information of surface chemical composition for different Sn foils were obtained by X-ray photoelectron spectrometry (XPS) (Thermo Scientific Nexsa). The existence of Sn cations in the electrolyte solution at the charged state was proven by energy-dispersive X-ray fluorescence (XRF) spectrometry (Bruker S2 PUMA). A quantitative analysis of the Sn cations in the charged electrolyte was carried out with inductively-coupled plasma optical emission spectroscopy (ICP-OES) (Thermo Fisher iCAP PRO). For the ICP-OES test, a Sn-Li battery was first charged to 20 mAh at the current of 5 mA (1 mA cm^{-2}) and then disassembled. All components in the pouch cell except for the cathode and anode (i.e. glass fibers, PIL/PP separator and electrolyte solution) were digested

completely with a mixed acid of hydrofluoric acid (HF) and aqua regia at 200°C. The treated solution was then diluted by water and then tested.

The charge-discharge profiles of the Sn-Li battery were obtained using a Neware battery tester. For the long-term cycling test, the Sn-Li battery was cycled at 0.2 mA cm⁻² with an areal charge capacity limitation of 0.1 mAh cm⁻² and a lower cutoff voltage of 2 V. For tests with higher current densities and larger areal capacity limitations, the cutoff voltage was reduced to 1.5 V to ensure completion of the reduction process. As the Sn foil is used as both the active material and current collector, a constant capacity limitation is applied to prevent complete dissolution of the current collector. In addition, as the charged capacity is fixed, the discharge capacity is proportional to the Coulombic efficiency of the battery.

Sn-Al batteries with PP and PIL/PP separators were utilized to investigate the surface composition of the anode after cycling and compare the ability of different separators to inhibit the adverse migration of Sn²⁺ from the catholyte to the anolyte and the side reactions between Sn²⁺ and Li metal at the anode. The cycled Al anodes from Sn-Al batteries were examined with XRD.

To study the effect of the type of metal on the charge-discharge mechanism at the cathode, batteries with Sn-Li, Cu-Li or Ni-Li were further charged and discharged at the current density of 0.4 mA cm⁻² with an areal capacity limitation of 0.4 mAh cm⁻² in a Binder climate chamber between 10 °C and 50 °C using a Bio-Logic MP3 potentiostat. The activation energies of the stripping (charging) process for the different metals were obtained from the change in average charge potential with temperature according to

Arrhenius equation. Scanning electron microscope (ZEISS EVO MA10) was used to examine the surface morphology of metal foils after cycling under different conditions. The cross-sectional SEM images were obtained with Thermo Fisher Scientific Quattro S environmental scanning electron microscope. Atomic force microscopy (AFM) images were acquired with Veeco MultiMode AFM.

Self-discharge tests were carried out to study the loss in capacity with time for batteries with different metal cathodes. Specifically, the batteries were charged to an areal capacity of 0.4 mAh cm^{-2} at a current density of 0.4 mA cm^{-2} , left at the charged state for different resting times from 0 h to 20 h, and then discharged to 1.5 V at the same current density. During rest, the transfer of metal cations across the separator will reduce the active species in the cell and decrease the discharge capacity that can be obtained.

Raman spectroscopy was utilized to investigate the solvation structure of the electrolyte from different metal-lithium batteries with WITec Alpha300R Raman system under the excitation laser of 532 nm wavelength. The tested electrolytes were prepared by charging different metal-lithium batteries to an areal capacity limitation of 4 mAh cm^{-2} (i.e. 20 mAh) and then collected by capillary tubes for testing.

Calculation of the number of electrons transferred for Cu cathode

After applying a charge capacity of 20 mAh, the mass of Cu is reduced from 0.2158 g to 0.1719 g. The measured specific capacity of Cu cathode is

$$Q_{\text{specific}} = \frac{Q_{\text{applied}}}{M_{0, \text{Cu}} - M_{t, \text{Cu}}} = \frac{20 \text{mAh}}{0.2158 \text{g} - 0.1719 \text{g}} = 455.6 \text{mAh g}^{-1}$$

During charging, if we assume Cu is oxidized to Cu^{n+} such that



Then the measured capacity of the redox reaction becomes

$$Q_{\text{Cu} \leftrightarrow \text{Cu}^{n+}} = \frac{1000nF}{3600M_{\text{Cu}}} = \frac{1000 * n * 96485}{3600 * 63.546} = 455.6 \text{ mAh } g^{-1}$$

$$n = 1.08 \approx 1$$

Therefore, Cu undergoes a one-electron transfer to Cu^+ .

Calculation of the number of electrons transferred for Ni cathode

After applying a charge capacity of 20 mAh, the mass of Ni is reduced from 0.2140 g to 0.1927 g. The measured specific capacity of Ni cathode is

$$Q_{\text{specific}} = \frac{Q_{\text{applied}}}{M_{0, \text{Ni}} - M_{t, \text{Ni}}} = \frac{20 \text{ mAh}}{0.2140 \text{ g} - 0.1927 \text{ g}} = 939.0 \text{ mAh } g^{-1}$$

During charging, if we assume Ni is oxidized to Ni^{n+} such that



Then the measured capacity of the redox reaction becomes

$$Q_{\text{Ni} \leftrightarrow \text{Ni}^{n+}} = 939.0 \text{ mAh } g^{-1}$$

$$n = 2.06 \approx 2$$

Therefore, Ni undergoes a two-electron transfer to Ni^{2+} .

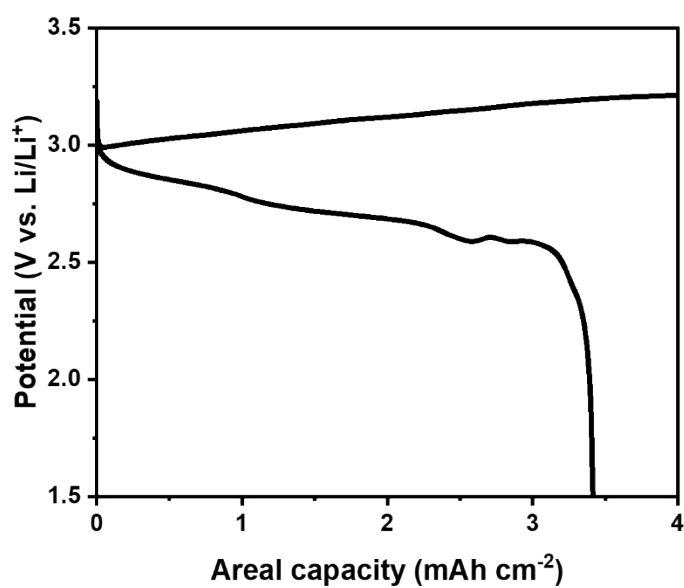


Figure S1 Charge/discharge curve of a Sn-Li battery at a current density of 1 mA cm^{-2} with an areal capacity limitation of 4 mAh cm^{-2} (total capacity of 20 mAh).

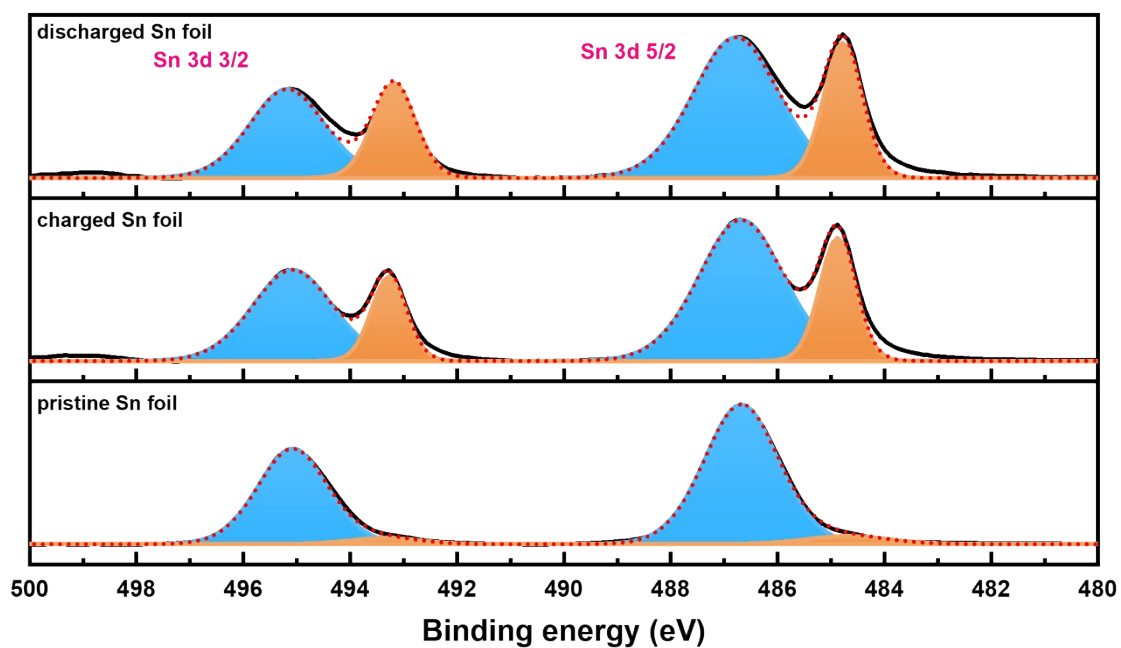


Figure S2 XPS spectra of pristine, charged, and discharged Sn foils.

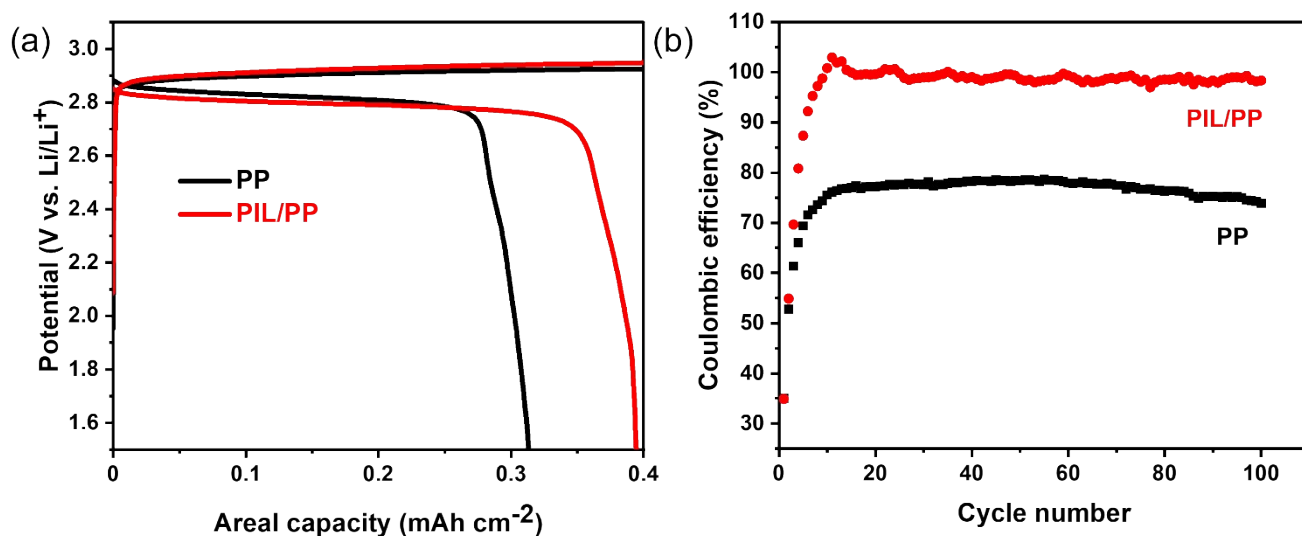


Figure S3 (a) Typical charge-discharge curves of Sn-Li batteries with PP or PIL/PP separator; (b) cycle performance of the corresponding Sn-Li battery.

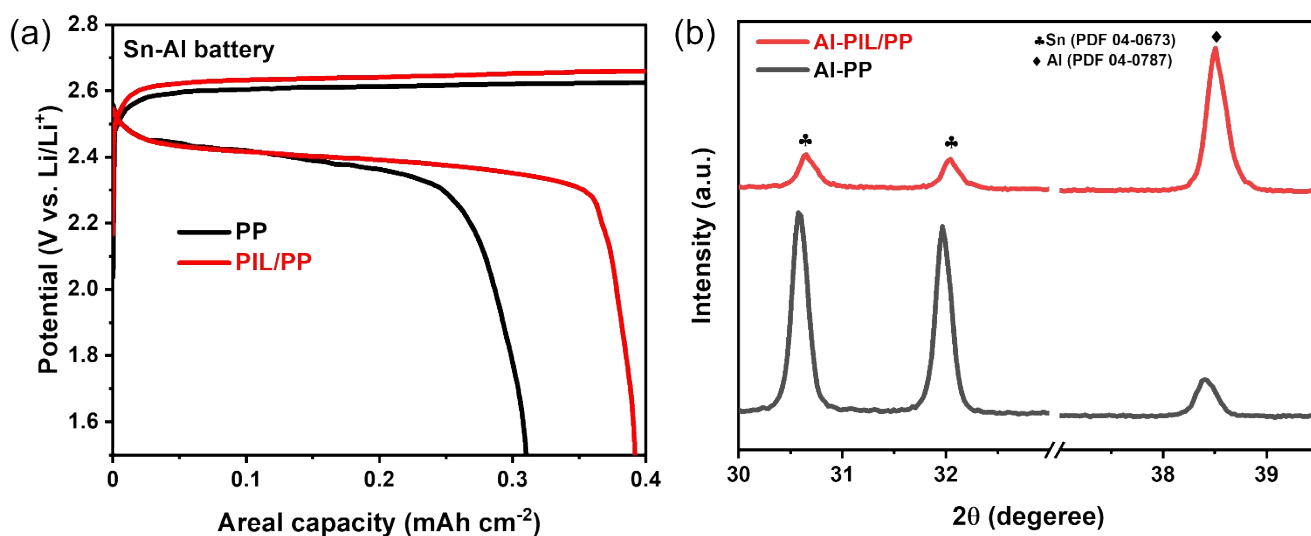


Figure S4 (a) Typical charge-discharge curves of Sn-Al batteries with PP or PIL/PP separator; (b) XRD pattern of Al foils after cycling for 20 cycles in Sn-Al batteries with PP or PIL/PP separator.

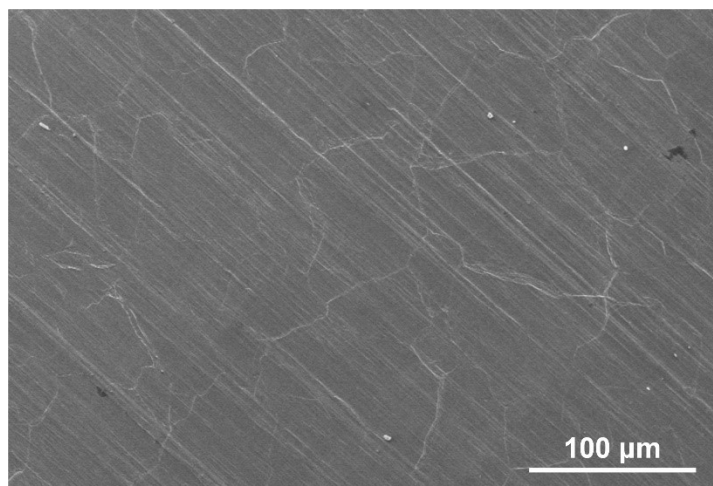


Figure S5 SEM image of the pristine Sn foil.

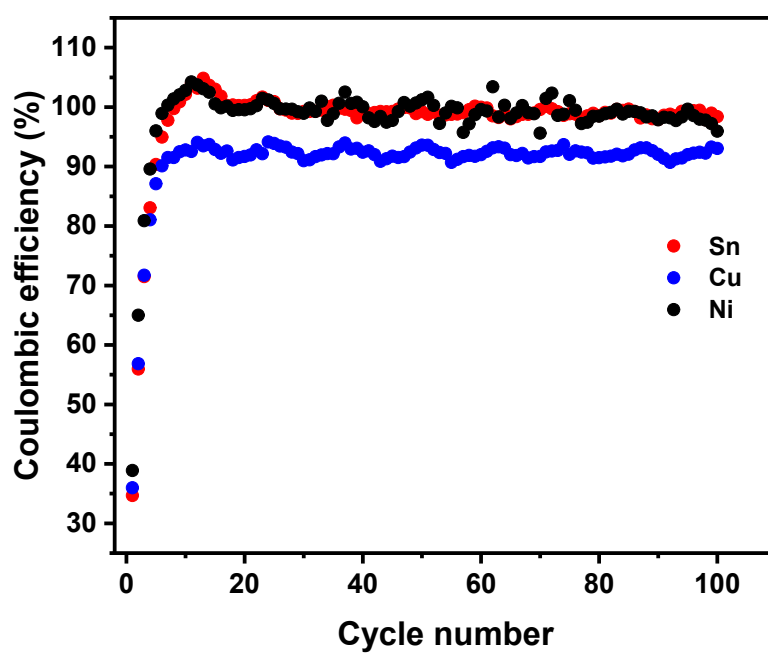


Figure S6 Coulombic efficiency of Sn-Li, Cu-Li and Ni-Li batteries with PIL/PP separator cycling at a current density of 0.4 mA cm^{-2} with an areal capacity limitation of 0.4 mA cm^{-2} .

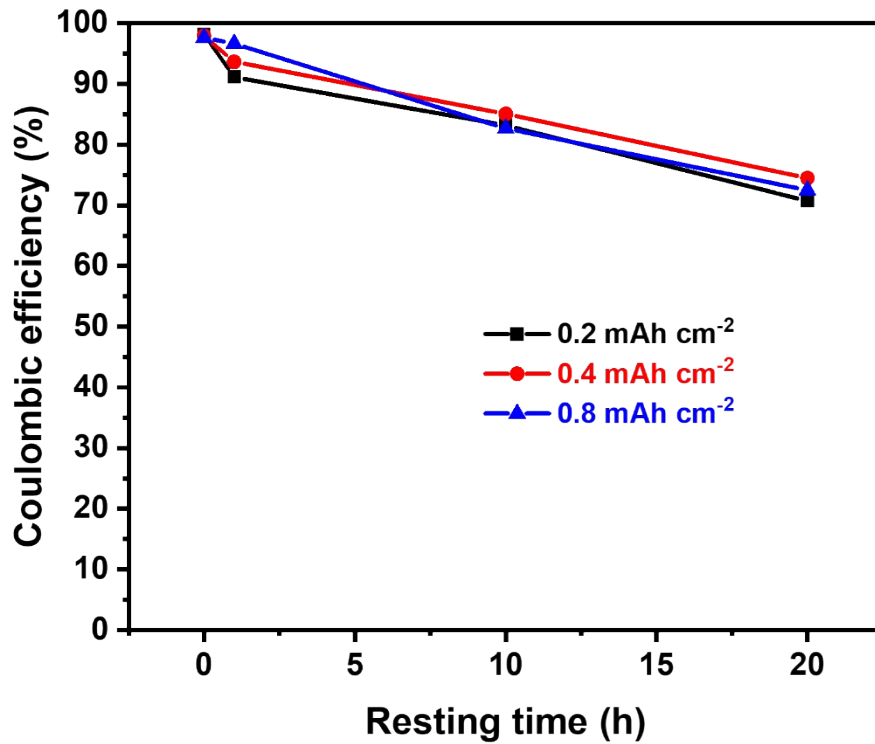


Figure S7 Coulombic efficiency of Sn-Li battery with different areal capacities after self-discharge tests with different resting times.

References :

1. K. Xue, Y. Zhao, P.-K. Lee and D. Y. W. Yu, *Energy & Environmental Materials*, in press. DOI: 10.1002/eem2.12395